

1 **CO<sub>2</sub> and CH<sub>4</sub> exchanges between moist moss tundra and atmosphere on Kapp**  
2 **Linne, Svalbard**

3 **Anders Lindroth<sup>1</sup>, Norbert Pirk<sup>2</sup>, Ingibjörg S Jónsdóttir<sup>3</sup>, Christian Stiegler<sup>4</sup>, Leif**  
4 **Klemedtsson<sup>5</sup>, and Mats B Nilsson<sup>6</sup>**

5 <sup>1</sup>Department of Physical Geography and Ecosystem Science, Lund University, Lund, Sweden.

6 <sup>2</sup>Department of Geosciences, University of Oslo, Oslo, Norway.

7 <sup>3</sup>Life and Environmental Sciences, University of Iceland, Reykjavik, Iceland.

8 <sup>4</sup>Bioclimatology, Georg-August Universität Göttingen, Göttingen, Germany.

9 <sup>5</sup>Department of Earth Sciences, University of Gothenburg, Gothenburg, Sweden.

10 <sup>6</sup>Department of Forest Ecology and Management, Swedish University of Agricultural Sciences,  
11 Umeå, Sweden.

12 Corresponding author: anders.lindroth@nateko.lu.se

## 13 Abstract

14 We measured CO<sub>2</sub> and CH<sub>4</sub> fluxes using chambers and eddy covariance (only CO<sub>2</sub>) from a moist  
15 moss tundra in Svalbard. The average net ecosystem exchange (NEE) during the summer (9  
16 June-31 August) was negative (sink) with  $-0.139 \pm 0.032 \mu\text{mol m}^{-2}\text{s}^{-1}$  corresponding to  $-11.8 \text{ g C}$   
17  $\text{m}^{-2}$  for the whole summer. The cumulated NEE over the whole growing season (day no. 160 to  
18 284) was  $-2.5 \text{ g C m}^{-2}$ . The CH<sub>4</sub> flux during the summer period showed a large spatial and  
19 temporal variability. The mean value of all 214 samples was  $0.000511 \pm 0.000315 \mu\text{mol m}^{-2}\text{s}^{-1}$   
20 which corresponds to a growing season estimate of  $0.04$  to  $0.16 \text{ g CH}_4 \text{ m}^{-2}$ . Thus, we find that  
21 this moss tundra ecosystem is closely in balance with the atmosphere during growing season  
22 when regarding exchanges of CO<sub>2</sub> and CH<sub>4</sub>. The sink of CO<sub>2</sub> as well as the source of CH<sub>4</sub> are  
23 small in comparison with other tundra ecosystems in high Arctic.

24  
25 Air temperature, soil moisture and greenness index contributed significantly to explain the  
26 variation in ecosystem respiration ( $R_{\text{eco}}$ ) while active layer depth, soil moisture and greenness  
27 index were the variables that best explained CH<sub>4</sub> emissions. Estimate of temperature sensitivity  
28 of  $R_{\text{eco}}$  and gross primary productivity (GPP) showed that the sensitivity is slightly higher for  
29 GPP than for  $R_{\text{eco}}$  in the interval  $0 - 4.5 \text{ }^\circ\text{C}$ , thereafter the difference is small up to about  $6 \text{ }^\circ\text{C}$  and  
30 then it began to raise rapidly for  $R_{\text{eco}}$ . The consequence of this, for a small increase in air  
31 temperature of 1 degree (all other variables assumed unchanged) was that the respiration  
32 increased more than photosynthesis turning the small sink into a small source ( $4.5 \text{ g C m}^{-2}$ ) during  
33 the growing season. Thus, we cannot rule out that the reason why the moss tundra is close to  
34 balance today is an effect of the warming that has already taken place in Svalbard.

## 35 1 Introduction

36 Climate warming is predicted to be most evident at high latitudes (Friedlingstein et al., 2006)  
37 with profound effects on ecosystem functioning. One of the high latitude regions that are  
38 expected to experience the most dramatic changes caused by climate change is the Arctic. This  
39 region which is located roughly north of the tree-line is characterized by cold winters and cool  
40 summers and with mean annual temperatures below zero. The summer periods are short ranging  
41 between 3.5 to 1.5 months from the southern boundary to the north and July is normally the  
42 warmest month. Annual precipitation is generally low decreasing from about 250 mm in the  
43 southern areas to 45 mm in polar deserts in the north (Callaghan et al., 2005).

44  
45 The permafrost soils in the Arctic store  $1035 \pm 150 \text{ Pg}$  of organic carbon in the top 0-3 m  
46 (Hugelius et al., 2014) which is more than the average 2010-2019 of 860 Pg of carbon in the  
47 atmosphere (Friedlingstein et al., 2020). The increased warming in these areas can induce higher  
48 decomposition rates due to increased microbial activity which will provide a positive feedback to  
49 the climate system (Schuur et al., 2015). On the other hand, warming can also increase  
50 photosynthesis and carbon uptake and thus compensate for, or exceed, the effect of increased  
51 decomposition. Climate warming is also affecting plant community composition and the length  
52 of the growing season (Post et al., 2009) which also has an impact on the processes regulating  
53 annual carbon emissions and uptake (Bosiö et al., 2014). There is however a large uncertainty  
54 regarding the timing, magnitude and possible sign of potential feedbacks caused by these  
55 changes (Myers-Smith et al., 2020).

56

57 Understanding processes that are controlling the exchanges of greenhouse gases in the Arctic is  
58 crucial for assessment of potential feedback effects. For this purpose, multiple year-around long-  
59 term studies including direct measurements of CO<sub>2</sub> and CH<sub>4</sub> fluxes covering all seasons, winter,  
60 spring, summer and autumn would be ideal. This is a great challenge in the harsh climate of the  
61 Arctic and with limited support of key infrastructures for, e.g., provision of electricity for  
62 operation of instruments.

63  
64 In spite of these difficulties a few year-around studies have been performed during the last  
65 couple of decades. In the low Arctic, Oechel et al. (2013) demonstrate the importance of the  
66 wintertime fluxes in a tussock tundra ecosystem in Alaska. They found that the non-summer  
67 season emitted more CO<sub>2</sub> than the corresponding uptake during the summer resulting in a net  
68 source to the atmosphere of about 14 g C m<sup>-2</sup> on an annual basis. They also showed that the  
69 shoulder seasons, spring and autumn roughly out-weighted the summer uptake. Euskirchen et al.  
70 (2012, 2016) measured net CO<sub>2</sub> exchange in three different tundra ecosystems; heath tundra,  
71 tussock tundra and wet sedge tundra in northern Alaska over three years. They found that the  
72 uptake of -51 to -95 g C m<sup>-2</sup> during the summer (June-August) was overturned by the respiration  
73 that occurred during the winter period resulting in net annual losses for all three ecosystems.  
74 Zhang et al. (2019) reported five years of year-around flux measurements in a heath ecosystem  
75 on west Greenland and they found that the heath was an annual sink of -35±15 g C m<sup>-2</sup>. One year  
76 with an anomalously deep snow pack showed a 3-fold higher respiration during the winter as  
77 compared to the other years which resulted in a significantly lower net uptake during that year.

78  
79 Even fewer studies have been done on year-around studies in the high Arctic. Lüers et al. (2014)  
80 quantified the annual CO<sub>2</sub> budget using eddy covariance measurements in a river catchment area  
81 near Ny-Ålesund on Spitsbergen in the Svalbard archipelago and they found that the ecosystem  
82 was in C-balance. The footprint area was a semi-polar desert with only 60% vegetation cover and  
83 patches of bare soil and stones. Also in Svalbard but further south in Adventdalen on a flat  
84 alluvial fen irregularly covered with ice wedged polygons, Pirk et al. (2017) made year-around  
85 measurements of CO<sub>2</sub> fluxes and found it to be a net sink of -82 g C m<sup>-2</sup>. Because of the  
86 irregularities caused by the ice wedges and the differences in wetness, they focused the analyses  
87 on the spatial variability in two different directions, one wetter and one drier, and they estimated  
88 the annual net ecosystem exchange to -91 g C m<sup>-2</sup> and -62 g C m<sup>-2</sup> for the respective areas.

89  
90 The Arctic ecosystems constitute also a source of CH<sub>4</sub> to the atmosphere even if it is not a very  
91 large one. Saunois et al. (2020) estimated that the Northern high latitude region (60°N - 90°N)  
92 contributed 4% of global emissions and emissions from wetlands are only part of the emissions  
93 from this region. However, in the light of the vulnerability of the high Arctic permafrost areas  
94 and considering the large carbon pool and the predicted changes in climate, a quantification and  
95 understanding of CH<sub>4</sub> exchanges in these areas are still important. Christensen et al. (2004)  
96 showed one example of a dramatic impact of the climate warming on the CH<sub>4</sub> emissions in a  
97 permafrost mire in sub-arctic Sweden. The warming which is visible in this area since decades  
98 and its impact on permafrost and vegetation changes was estimated to have caused an increase of  
99 landscape CH<sub>4</sub> emissions in the range 22-66% in the period 1970 to 2000.

100  
101 Mastepanov et al. (2008) were the first to show the importance of emissions also outside of the  
102 growing season. They observed a large burst of CH<sub>4</sub> from a fen area in Zackenberg, Greenland

103 after the growing season and during the time when the soil started to freeze. This finding was  
104 confirmed in a later paper (Mastepanov et al., 2013) and the process was hypothetically  
105 attributed to the subsurface CH<sub>4</sub> pool. Hydrology and vegetation composition play an important  
106 role for CH<sub>4</sub> emission and dynamics. McGuire et al. (2012) made a comprehensive summary of  
107 CH<sub>4</sub> exchanges of the Arctic tundra showing the difference between wet and dry ecosystems; the  
108 wet tundra emitted 5.4 to 13.0 g CH<sub>4</sub>-C m<sup>-2</sup> during summer and 8.5 to 20.2 g CH<sub>4</sub>-C m<sup>-2</sup>  
109 annually. The corresponding values for the dry/mesic tundra were 0.3 to 1.4 g CH<sub>4</sub>-C m<sup>-2</sup> and 0.3  
110 to 4.3 g CH<sub>4</sub>-C m<sup>-2</sup>, respectively. Bao et al. (2021) utilized year-around measurements of CH<sub>4</sub>  
111 fluxes from three sites of the Ameriflux network in Northern Alaska to demonstrate the  
112 importance of the spring and autumn seasons for the annual emission. The shoulder seasons  
113 contributed about 25% of the annual emissions and the autumn season had about three times  
114 higher emission than the spring season. These findings increasingly emphasise the importance of  
115 year-around measurements to fully understand the CH<sub>4</sub> controls and dynamics.  
116

117 The main aim of this study is to provide another piece of the puzzle concerning CO<sub>2</sub> and CH<sub>4</sub>  
118 exchanges from different but widespread ecosystem types in the high Arctic. We hypothesise  
119 that this moist tundra ecosystem is a net carbon sink during the growing season and that the  
120 summer emissions of methane will be at levels comparable with other methane emitting high  
121 Arctic ecosystems. We made flux measurements of CO<sub>2</sub> and CH<sub>4</sub> in an moist moss tundra  
122 ecosystem situated at Kapp Linne on the west coast of the Svalbard archipelago in 2015 and with  
123 an additional campaign in 2016. The measurements in 2015 were done using both eddy  
124 covariance system (CO<sub>2</sub>) and chambers (CO<sub>2</sub> and CH<sub>4</sub>) but only chambers in 2016. We quantify  
125 ecosystem respiration (R<sub>eco</sub>), gross primary productivity (GPP) and net ecosystem exchange  
126 (NEE) during the growing season based on a combination of chamber end eddy covariance  
127 measurements. The CH<sub>4</sub> emission was only quantified for the summer season. We also analyze  
128 the environmental controls of the fluxes.

## 129 **2 Materials and Methods**

### 130 **2.1 Research site and measurements**

131  
132 This study was performed in the Svalbard archipelago near the weather station Isfjord Radio  
133 (78°03'08" N 13°36'04" E, alt. 7 m) which is located right on the foreland of Kapp Linné on the  
134 island of Spitzbergen (Fig. S1). The tundra area where the measurements were performed is  
135 located about 1 km southeast of the station. The study area consists of moist moss tundra, a  
136 widespread ecosystem in Svalbard (Vanderpuye et al., 2002; Ravolainen et al., 2020). The  
137 vegetation is characterised by the moss species *Tomentypnum nitens*, *Sanionia uncinata* and  
138 *Aulacomium palustre* and a sparse cover of vascular plants (20-40%), dominated by *Equisetum*  
139 *arvense*, *Salix polaris* and *Bistorta vivipara*. Other vascular plant species found in the plots:  
140 *Saxifraga cespitosa*, *Saxifraga oppositifolia*, *Silene acaulis*, and some grass species, most likely  
141 *Alopecurus ovatus* (previously *A. borealis*), and *Poa arctica*. The vegetation analysis was made  
142 from photographs of chamber location plots taken between 26 June and 2 July 2015 (see Figs.  
143 S4a-4y in Supplement).  
144

145 The net ecosystem exchange of CO<sub>2</sub> was measured with an eddy covariance (EC) system located  
146 centrally on the moss tundra (78°03'28.6" N 13°38'40" E). The sonic anemometer (USA-1;

147 Metek GmbH, Germany) was mounted on top of a tripod (see Fig. S1) at 2.7 m height. The CO<sub>2</sub>  
148 and H<sub>2</sub>O concentrations were measured with an open path sensor (LI-7500; Li-Cor Inc., USA)  
149 placed just beneath the sonic and inclined about 30° pointing towards east. Radiation  
150 components, incoming and outgoing short-wave and long-wave (CNR-4; Kipp & Zonen, the  
151 Netherlands) were measured at 2.0 m height above ground with the sensor directed towards  
152 south. All sensors were connected to a datalogger (CR-1000; Campbell Scientific, USA) which  
153 was powered by a solar panel and a battery. The EC sensors were sampled and stored at 10 Hz  
154 and all other sensors were sampled at 0.1 Hz with storage of 30 min mean values. These  
155 measurements were made from 25 June to 17 September 2015. The total data coverage during  
156 this period was 47% with a longer break in the measurements between 28 July and 29 August.

157 The impact of substantial gap filling of measured EC data and partial modelling in order to  
158 complete the full growing season is further discussed below.  
159

160 The soil efflux of CO<sub>2</sub> and CH<sub>4</sub> was measured with a dark chamber connected to a gas analyzer  
161 (Ultraportable Greenhouse Gas Analyzer; Los Gatos Research, USA) on 24 locations within the  
162 EC average footprint area. A circular thin-steel frame, 15 cm in diameter and 15 cm high, was  
163 inserted ca 5 cm into the ground in each location. The sharp edge of the frames made it easy to  
164 insert them into the ground without damaging the vegetation and with minimal soil disturbance.  
165 A picture was taken of each frame (see Supplement) for documentation of vegetation and for  
166 calculation of different indexes. The chamber was also made from steel and it had a rubber seal  
167 in the end facing the frame (Fig. S2) to make it air tight when mounted on the frame. The volume  
168 of the chamber and the part of the frame raised above the surface was 5.3 L. A small fan was  
169 installed inside the chamber to provide good mixing of the air during measurement. A small  
170 weight (stone) was placed on top of the chamber during measurement to prevent it from moving  
171 due to wind gusts. During concentration measurement air was circulated in a closed loop  
172 between the chamber and the gas analyzer in ca. 10 m long 4 mm diameter polyethene tubes (see  
173 Fig. S2). The air flow through the analyzer was ca 1.2 L min<sup>-1</sup>. The chamber was ventilated in  
174 the free air about 1 minute before each measurement which lasted for 5 minutes. The  
175 concentrations were recorded and stored once per second by the gas analyzer. The time stamp of  
176 the recorded data was used to identify measurement cycles for analysis of fluxes.

177  
178 The chamber measurement positions were selected in the following way. The frames were  
179 grouped in two sections, one north-east and one south-west of the flux tower since it was  
180 expected that the main wind direction would be along that direction. Each group was then split  
181 into three subsections with four measurement points within each one of them. The locations were  
182 named S1:1-S1:4, S2:1-S2:4, S3:1-S3:4, N1:1-N1:4, N2:1-N2:4 and N3:1-SN3:4. The four  
183 measurement points within each subsection were then placed along a transect with 3-4 m  
184 between each point. This way it was possible to measure all four chamber locations without  
185 having to move the whole measurement system. Chamber measurements were made in three  
186 separate campaigns: mid-summer (26 June to 2 July 2015), late-summer (25-27 August 2015)  
187 and early-summer (14-15 June 2016). Each location was measured three times during each one  
188 of the three campaigns, a total of 216 measurements. Besides gas concentrations, also soil  
189 temperature (5 cm), soil moisture (0-5 cm) and active layer depth was measured during each  
190 campaign.

191

192 Meteorological data needed for analyses and gap-filling were obtained as follows: Hourly air  
193 temperature and relative humidity from Isfjord radio, half-hourly global radiation from  
194 Adventdalen, daily snow depth and ground ice conditions from Svalbard airport and monthly  
195 precipitation from Isfjord radio and Barentsburg. The distance between the measurement site and  
196 these stations are; Isfjord radio, 1 km, Barentsburg, 13 km, Svalbard airport, 46 km and  
197 Adventdalen, 50 km. Using data from the more distant locations, Svalbard airport and  
198 Adventdalen, introduces some additional uncertainty. Concerning global radiation data we could  
199 compare in situ measured half-hourly radiation with the corresponding data from Adventdalen  
200 for a shorter period and it showed general good agreement although with relatively large scatter  
201 ( $y = 0.84x + 15.9$ ;  $r^2=0.57$ ;  $n=580$ ). According to Dobler et al. (2021) the amount of precipitation  
202 in the area where Kapp Linne and Svalbard airport are located don't show any significant  
203 differences on an annual basis. Vickers et al. (2020) analysed timing of snow cover in Svalbard  
204 and they show that the mean (2000-2019) first snow-free day is very similar in areas where Kapp  
205 Linne and Svalbard airport are located. Thus, we are confident that using data from these  
206 relatively remote locations does not introduce serious bias in our analyses. Data sources are  
207 given in Acknowledgement.

208

### 209 3. Data analysis

210

211 The rawdata from the eddy covariance flux measurements were analysed using the Eddypro  
212 software version 6.1.0 (Li-Cor, 2016). Correction was made for the impact of the additional heat  
213 flux in the sensor path of the open path analyzer on the flux calculations according Burba et al.  
214 (2008). Gap filling during the measurement period was made using the REdyProc online eddy  
215 covariance data processing tool developed at the Max Planck Institute for Biogeochemistry  
216 (Wutzler et al., 2018) without  $u^*$  correction since we could not identify any threshold for  $u^*$ . The  
217  $u^*$  threshold is generally low for low and smooth vegetation (Pastorello et al., 2020) and for a  
218 wind exposed site as ours, it is not surprising that such threshold could not be found. Flux  
219 partitioning was made with the daytime-based method according Lasslop et al. (2000). Only data  
220 of highest quality, i.e. class=0 was retained for the gap filling and further analyses. Gap filling  
221 outside of the EC measurement period to obtain the carbon balance for a full growing season was  
222 made by modeling using the Lloyd & Taylor (1994) model for empirical relationships for  $R_{eco}$   
223 and an empirical light response function for GPP (see below). The measured respiration by  
224 chambers was used to obtain the parameters for  $R_{eco}$  and EC data was used for fitting of the light  
225 response function for GPP.

226

227 For flux footprint calculations the roughness length ( $z_0$ ) is needed and it was calculated from the  
228 wind profile relationship in near neutral ( $-0.01 < z/L < 0.01$ ) conditions:

229

$$230 \quad z_0 = \frac{z_m}{e^{(u(z) \frac{k}{u^*})}} \quad (1)$$

231

232 where  $z_m$  is measurement height,  $u(z)$  is wind speed at height  $z$ ,  $k$  is von Karman's constant and  
233  $u^*$  is friction velocity. We used the flux footprint prediction (FFP) online tool by Kjun et al.  
234 (2015) to calculate the footprint climatology.

235

236 The fluxes from the chamber measurements were estimated from the time change of the  
237 concentrations using linear regression. Every individual measurement was inspected and

238 evaluated manually. These inspections showed that 50 seconds for CO<sub>2</sub> and 100 seconds for CH<sub>4</sub>  
 239 were optimal to obtain near perfectly linear responses a few seconds after the chamber had been  
 240 placed on the frame. The slopes of the regressions were then used to calculate fluxes per unit  
 241 surface area. The flux detection limits for CO<sub>2</sub> and CH<sub>4</sub> were calculated in the following way:  
 242 first the peak-to-peak variation in the respective gases were determined when the chamber was  
 243 ventilated in the free air and when conditions were steady. Then 20 sets of artificial ‘fluxes’ for  
 244 each gas species were estimated based on 100 randomly generated concentrations for each data  
 245 set. The peak-to-peak difference was used as seed (input) for the randomly generated values. The  
 246 95% value of the distribution of these randomly generated fluxes was taken as the flux detection  
 247 limit for the respective gas.

249 The pictures of the vegetation inside of the chamber frames were analysed using the ImageJ  
 250 (<https://imagej.net>) public domain software. The camera color channel information (digital  
 251 numbers for Red (R), Green (G) and Blue (B) channels) was collected from the JPEG pictures.  
 252 This type of pictures is for instance used in studies that are tracking the phenological  
 253 development of vegetation (e.g. Richardson et al., 2009). The so-called green index (GI) is  
 254 applied to detect differences in greenness of vegetation:

$$256 \quad GI = G/(R+G+B) \quad (2)$$

258 This index was also estimated for the central footprint area (100 m radius) of the flux  
 259 measurement location using a picture taken at 160 m above the altitude of the measurement area.

260 Forward stepwise linear regression (Sigmaplot 12.5) was used to analyze the dependency of the  
 261 CO<sub>2</sub> and CH<sub>4</sub> fluxes on environmental variables. We tested for air temperature (T<sub>a</sub>), soil moisture  
 262 (θ), soil temperature (T<sub>s</sub>), active layer depth (ALD), measurement location (S<sub>id</sub>) and GI.

264 For gap filling of R<sub>eco</sub> we only had access to air temperature with full annual coverage and, thus,  
 265 we could only use this driver for estimation of the R<sub>eco</sub>. The measured chamber CO<sub>2</sub> fluxes were  
 266 fitted to the Lloyd & Taylor (1994) model with air temperature (T<sub>a</sub>) as independent variable:

$$268 \quad FCO_2 = a \cdot e^{b \left( \frac{1}{56.02} - \frac{1}{T_a + 46.02} \right)} \quad (3)$$

270 During the EC measurement period (25 June to 17 September 2015) the GPP was estimated as:

$$272 \quad GPP = NEE_f - R_{eco} \quad (4)$$

274 Where NEE<sub>f</sub> is the gap filled NEE according to Wutzler et al. (2018). This way R<sub>eco</sub> and GPP  
 275 become consistent with the measured and gap filled NEE. For the time before and after this  
 276 period NEE was estimated as the sum of modelled R<sub>eco</sub> and modelled GPP. The data for the GPP  
 277 model was derived from:

$$279 \quad GPP_m = NEE_m - R_{eco} \quad (5)$$

281 Where NEE<sub>m</sub> is the measured net ecosystem exchange. The GPP<sub>m</sub> was then fitted to a light  
 282 response function:

283  
284 
$$GPP_m = c1 + c2 \cdot c3 / (c2 + R_g) \quad (6)$$

285

## 286 **4 Results**

287 For CO<sub>2</sub> exchanges and partitioning we combined the soil efflux measurements with the chamber  
288 system with the eddy covariance flux measurements. This was crucial for the partitioning and for  
289 gap filling because from 20 April to 20 August at this location the sun is above the horizon 24  
290 hours of the day and this means that there were few occasions of dark nighttime measurements  
291 with the eddy covariance system and all of these were collected at the very end of the summer.  
292 We consider the chamber measurements that were distributed across the summer to be more  
293 representative of R<sub>eco</sub> for this location.

294

295 For CH<sub>4</sub> exchanges we don't have any eddy covariance measurements so we present only  
296 chamber data for this variable.

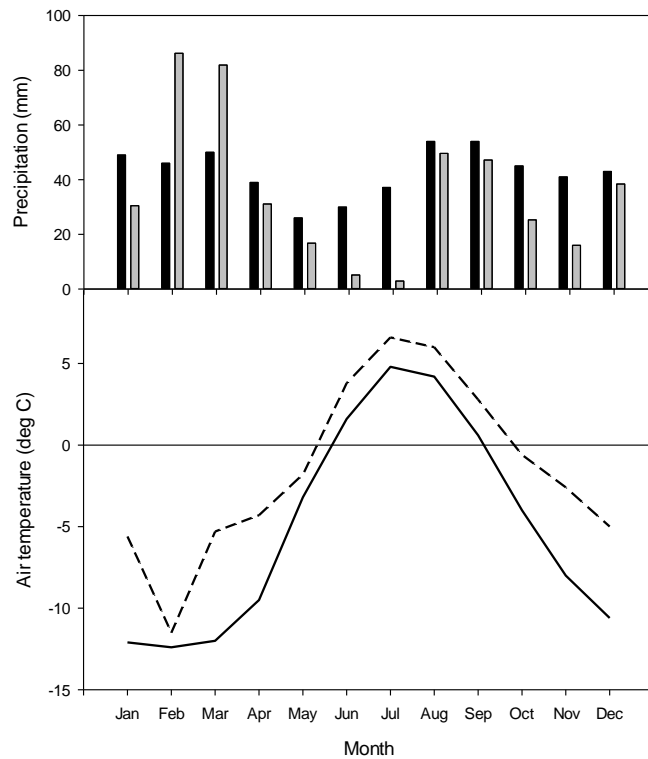
297

### 298 **4.1 Weather**

299

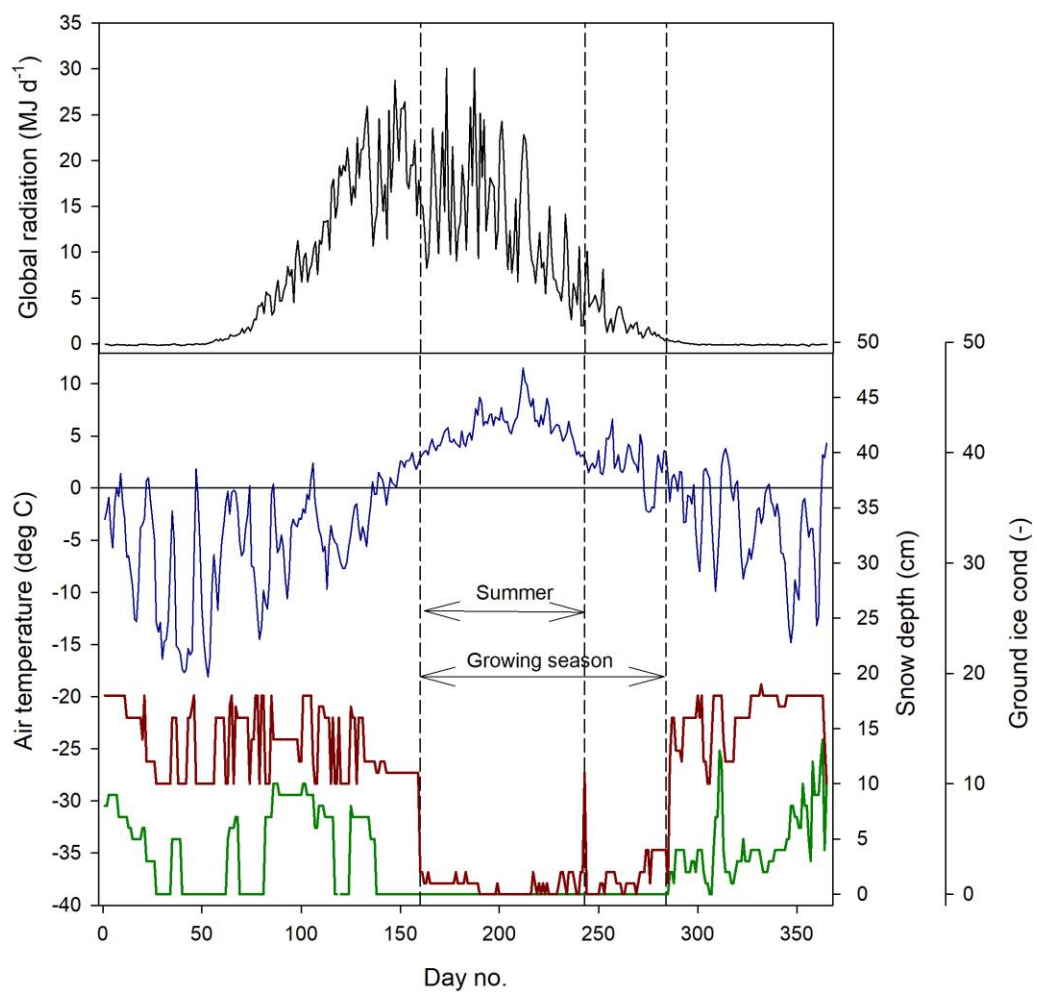
300 The mean annual temperature at Kapp Linne was -1.5 °C during 2015 which was 3.5 °C higher  
301 than the long-term mean (1961-1990) of -5.1 °C. The summer (June-August) mean of 5.5 °C was  
302 2.0 °C higher than the long-term mean for the same time period (Fig. 1). The summer  
303 precipitation in 2015 was much lower, 58 mm as compared to the long-term precipitation which  
304 was 121 mm. The annual precipitation was also lower, 431 mm compared to the long-term  
305 precipitation which was 514 mm.





306  
 307 Figure 1. Monthly precipitation (top): Long-term average 1961-1990 black bars and 2015 grey  
 308 bars. Data from Barentsburg for January-May, from Isfjord Radio for June-December. Mean  
 309 monthly air temperature (bottom): Solid line is long-term average 1961-1990 and dotted line is  
 310 2015. Data from Isfjord Radio which is located about 1 km west of the investigation area.

311  
 312 We defined the growing season (the period during which vegetation is photosynthesizing) based  
 313 on the permanence of the snow pack which resulted in start day no. 160 and end day no. 284  
 314 (Fig. 2). The summer period which normally is defined as June through August was here defined  
 315 as lasting between 9 June (same as start of growing season) until end of August (Fig.2).  
 316



317  
 318  
 319  
 320

Fig. 2 Weather conditions during 2015. Top panel: Mean daily global radiation at Adventdalen. Bottom panel: Mean daily air temperature at Isfjord Radio (blue), snow depth (red) and ground

321 ice conditions (green) at Svalbard airport close to Longyearbyen. The ground ice condition is  
322 scaled from 0 to 20 where 0 is no snow or ice on the ground and 20 indicate a complete cover of  
323 snow or ice.

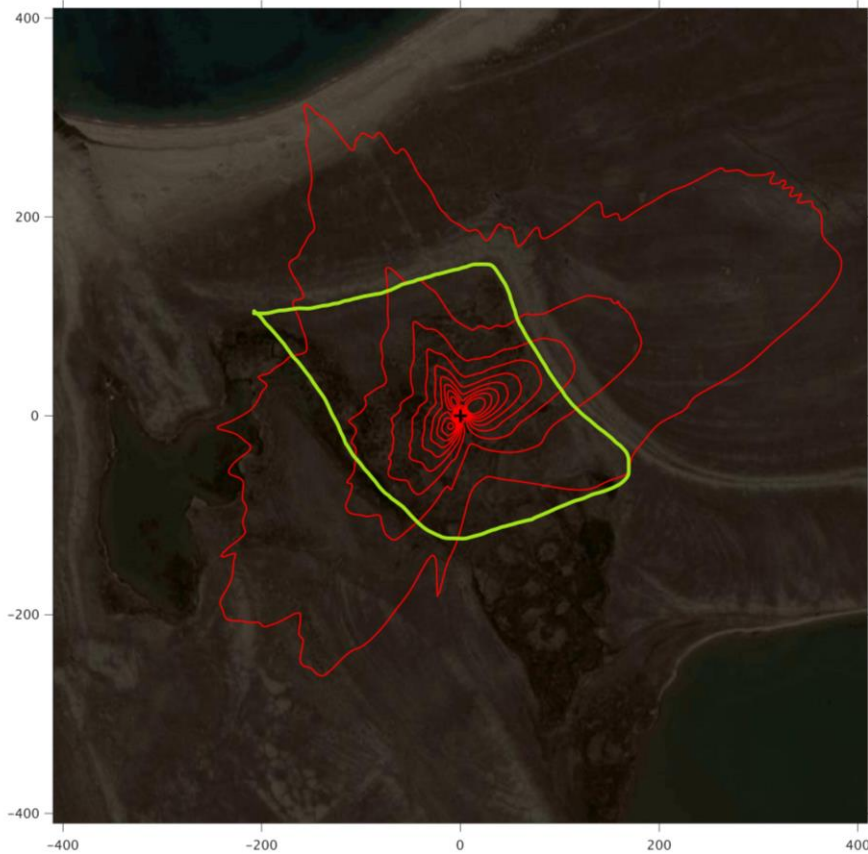
324

#### 325 4.2 Flux footprint and greenness

326

327 The footprint climatology shows a good representativity of the moss tundra surface by the EC  
328 measurements with 60-70% of fluxes emanating from areas well within the border of the tundra  
329 (Fig. 3). The mean green index for a circular area with radius of 100 m centered at the flux tower  
330 was 0.34 which corresponded exactly to the mean value for all chamber locations. The GI for the  
331 24 chamber locations varied between 0.316 and 0.369. We observed a good (visual) correlation  
332 between GI and coverage of green plants (see Figures S4a-S4y of chamber location pictures and  
333 GI).

334



335

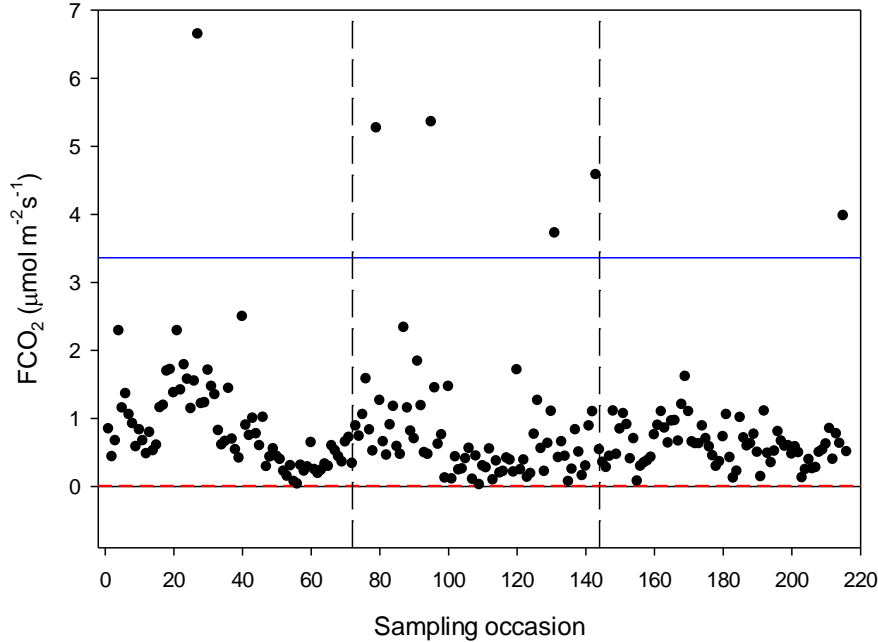
336 Figure 3. The footprint climatology with red contour lines 10-90%. The area within the green  
337 line mark the heart of the moss tundra. The scale (m) is shown on the outer borders of the  
338 picture.

339

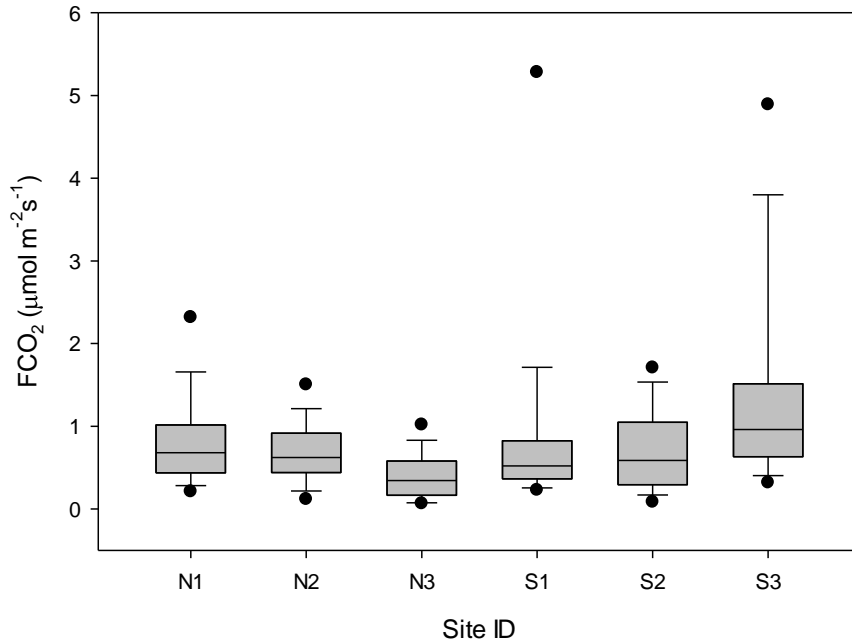
#### 340 4.3 CO<sub>2</sub> exchanges

341

342 The CO<sub>2</sub> fluxes from the chamber measurements showed quite large variation over time (Fig. 4)  
343 and across sampling locations (Fig. 5). The mean CO<sub>2</sub> flux of all samples was  $0.81 \pm 0.11 \mu\text{mol}$   
344  $\text{m}^{-2}\text{s}^{-1}$ . The uncertainty is given as the 95 confidence limit.  
345



346  
347 Figure 4. Measured CO<sub>2</sub> exchange (FCO<sub>2</sub>) from the 24 sampling points using dark chamber and  
348 portable gas analyzer. The dashed red line indicates CO<sub>2</sub> flux detection limit and the blue line  
349 represents 3xS.D. of all data points. The dashed vertical lines separate sampling periods from left  
350 to right: 14-15 June, 26 June – 2 July and 25-27 August, respectively.



351

352 Figure 5. Box plot of CO<sub>2</sub> fluxes (FCO<sub>2</sub>) per sampling location named N1-N3, S1-S3. The  
 353 boundaries of the grey boxes represent the 25% and 75% percentiles, the line represent the  
 354 median, whiskers above and below the boxes indicate the 10% and 90% percentiles. Outlying  
 355 points are also shown.

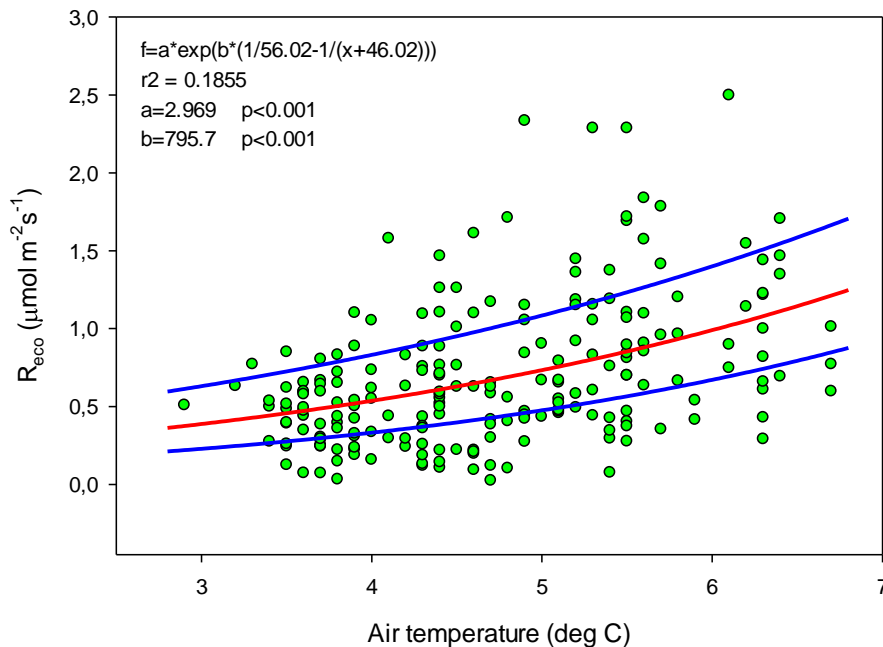
356  
 357 Of the tested environmental variables T<sub>a</sub>, θ, T<sub>s</sub>, ALD, S<sub>id</sub> and GI it was only T<sub>a</sub>, θ and GI that  
 358 contributed positively and significantly in decreasing order to explain the variability of the CO<sub>2</sub>  
 359 flux (Table 1).

360  
 361 Table 1. Result of stepwise linear regression with CO<sub>2</sub> flux as dependent variable. Normality test  
 362 failed but significance in all variables was confirmed with Wilcoxon Signed rank tests. T<sub>a</sub> is air  
 363 temperature, θ is soil moisture and GI is green index.

364

Variable	Partial-R <sup>2</sup>	Probability (p)
T <sub>a</sub>	0.190	<0.001
θ	0.037	0.002
GI	0.023	0.002

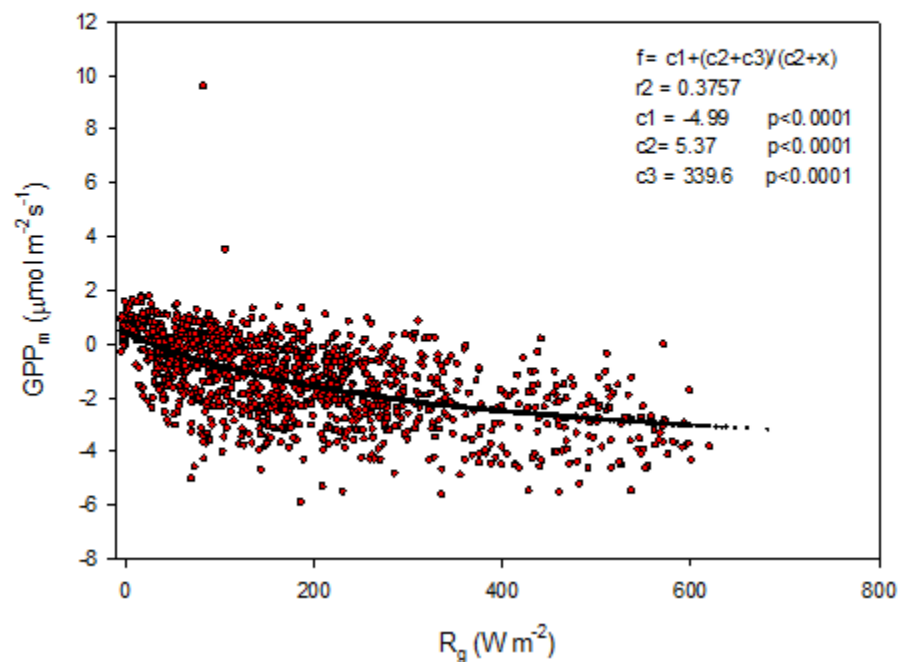
365  
 366 Ideally all of these variables should be used in a model to estimate R<sub>eco</sub> for gap filling purposes  
 367 but we could only use air temperature since this was the only variable that we had access to with  
 368 complete coverage for a full year. The Lloyd & Taylor model (Eq. 3 & Fig. 6)) was thus used to  
 369 estimate ecosystem respiration for 2015 using half-hourly air temperature as input.



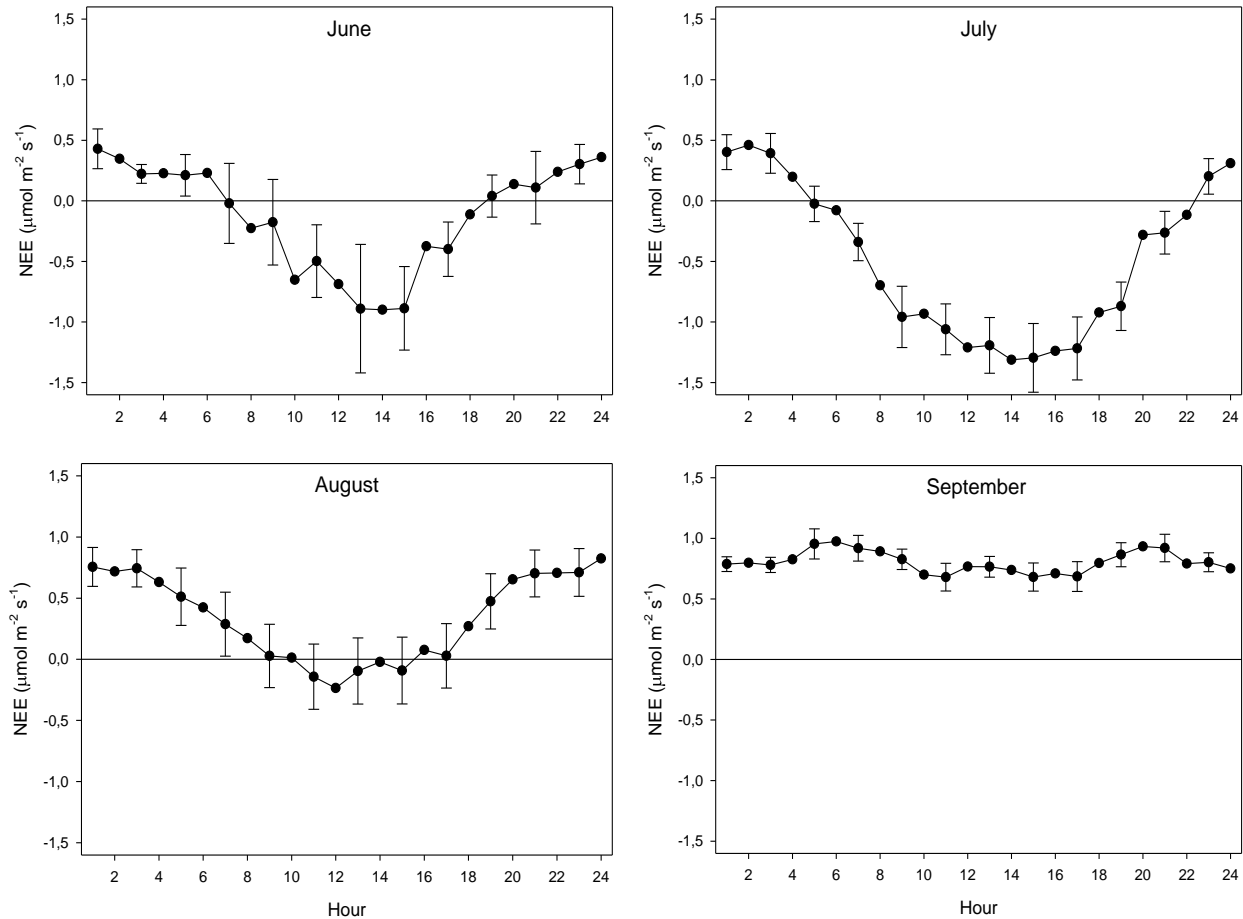
370  
 371 Figure 6. Measured ecosystem respiration (R<sub>eco</sub>; green dots) using chambers plotted against air  
 372 temperature. The red curve is the fitted equation and the blue curves are the corresponding  
 373 boundaries when considering the standard deviation of the parameters.

374

375 The modelled gross primary productivity (Eq. 6;  $GPP_m$ ) had a small offset when global radiation  
376 was zero (Fig. 7). This offset was adjusted for when the model was applied for gapfilling so that  
377  $GPP$  become zero during nighttime.



378  
379  
380 Figure 7. Gross primary productivity ( $GPP_m$ ) plotted against global radiation ( $R_g$ ) ; red symbols  
381 are estimated values according to eq. (5) and the black symbols are the fitted model.  
382  
383  
384  
385  
386

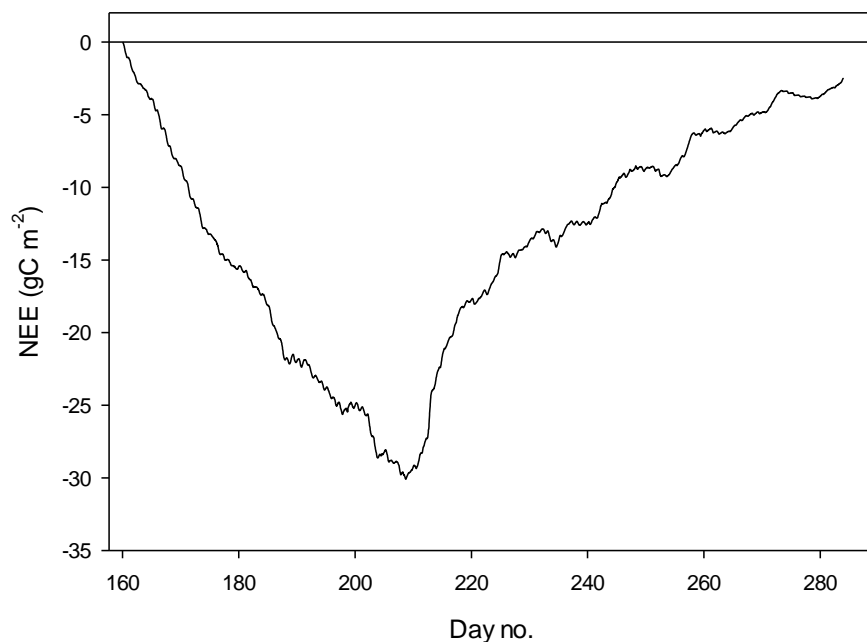


387  
 388 Figure 8. The mean monthly diurnal course of net ecosystem exchange (NEE) during the period  
 389 of eddy covariance measurements 25 June to 17 September. The error bars (every 2<sup>nd</sup> shown) are  
 390 the 95% confidence interval. Notice that the main part of August was gap filled because of  
 391 measurement problems.

392  
 393  
 394 The diurnal course of NEE during June - August exhibit the normal pattern with a successively  
 395 increasing drawdown of CO<sub>2</sub> during first half of the day resulting in a maximum around noon. It  
 396 should be noted that during June until 20 August the sun was over the horizon 24 hours, thus no  
 397 dark period. The positive values at the beginning and end of the diurnal courses are a result of  
 398  $R_{eco}$  being larger than GPP. As pointed out in Fig. 8, most of the data of August were gapfilled  
 399 causing some additional uncertainty. However, the diurnal course seems reasonable although the  
 400 peak during noon is much lower as compared to July. This can be explained by the much lower  
 401 incoming radiation in August as compared to July; the mean global radiation in July was 192 W  
 402 m<sup>-2</sup> and 98 W m<sup>-2</sup> in August. The mean air temperature was similar during July and August. In  
 403 September the incoming radiation is very low and thus GPP is also very low which result in a  
 404 NEE that is dominated by the  $R_{eco}$ . The positive NEE values around mid-night during June –  
 405 September are in good accordance with the values from the independent dark chamber  
 406 measurements (Fig. 5).

407

408 In order to assess the impact of the large gap in measured data in August where we only had two  
 409 days of measured fluxes at the end of the month we made a comparison between the gap filled  
 410 diurnal course based on Wutzler et al. (2018) respectively our modelling using Eqs. 3 & 6. The  
 411 results show very good agreement between the two methods (see Supplement) giving support to  
 412 the realism and reliability of the gap filled data.  
 413



414  
 415 Figure 9. The cumulated half-hourly net ecosystem exchange (NEE) during growing season.  
 416

417 The mean net CO<sub>2</sub> flux during the growing season was  $-0.019 \pm 0.024 \mu\text{mol m}^{-2}\text{s}^{-1}$  with  
 418 uncertainty given as the 95% confidence limit. The cumulated NEE during growing season  
 419 ended up negative with  $-2.5 \text{ g C m}^{-2}$  (Fig. 9). The mean net CO<sub>2</sub> flux during summer was  $-$   
 420  $0.139 \pm 0.032 \mu\text{mol m}^{-2}\text{s}^{-1}$  (95% confidence limit) and the cumulated NEE was  $-11.8 \text{ g C m}^{-2}$   
 421 (Table 2).  
 422

423 Table 2. Summary of seasonal C-fluxes from Kapp Linne. R<sub>eco</sub> is ecosystem respiration, GPP is  
 424 gross primary productivity and NEE is net ecosystem exchange.  
 425

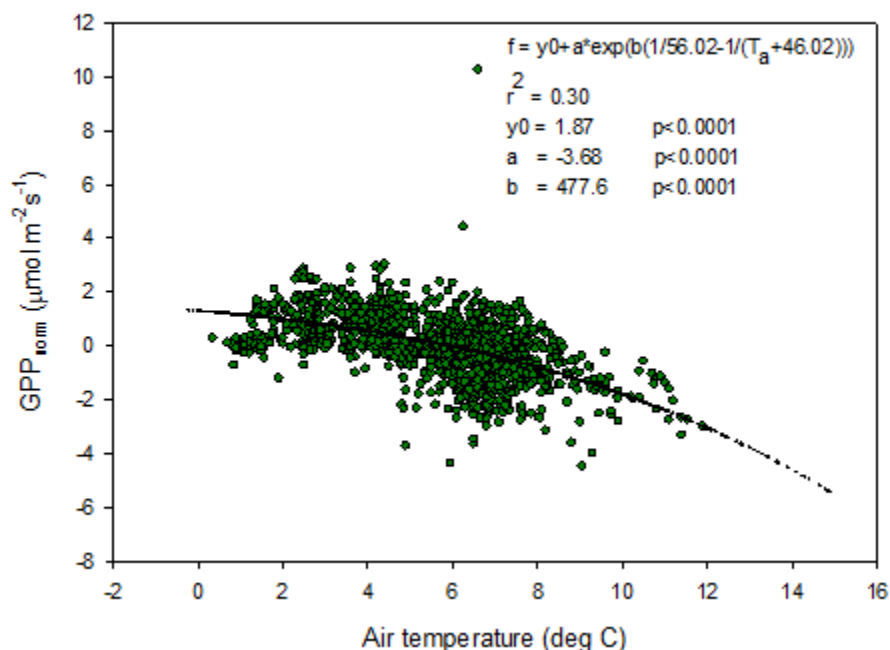
Period	Component	Value (gC m <sup>-2</sup> )
Growing season	Reco	110.2
	GPP	-112.7
	NEE	-2.5
Summer	Reco	94.1
	GPP	-105.9
	NEE	-11.8

426  
 427 4.4 Temperature sensitivity of R<sub>eco</sub> and GPP



428

429 The temperature sensitivity of the  $R_{eco}$  is already given by the fitted Lloyd & Taylor (1994)  
430 equation. In the absence of long time series of measurements during multiple year were natural  
431 climate variability could be used to assess temperature sensitivity of GPP we approached this  
432 problem in the following way. We normalize GPP for its dependence on radiation by estimating  
433 the difference between the 'measured' GPP and the model which only depends on radiation (see  
434 Fig. 7). A stepwise linear regression with normalized GPP as dependent variable and air  
435 temperature, time of season and vapour pressure deficit as independent variables, showed that of  
436 the total explained variance, air temperature stood for 94% and time of season and and vapour  
437 pressure deficit for 3% each. Thus, the resulting normalized GPP show effectively a dependence  
438 on air temperature (Fig. 10) with values becoming more negative, i.e. showing increasing GPP  
439 with increasing temperature. We fitted the same type of model to these data as for the  $R_{eco}$  to be  
440 able to compare sensitivities to temperature.



441

442 Figure 10. Normalized gross primary productivity (GPP) plotted against air temperature and with  
443 the fitted exponential model.

444

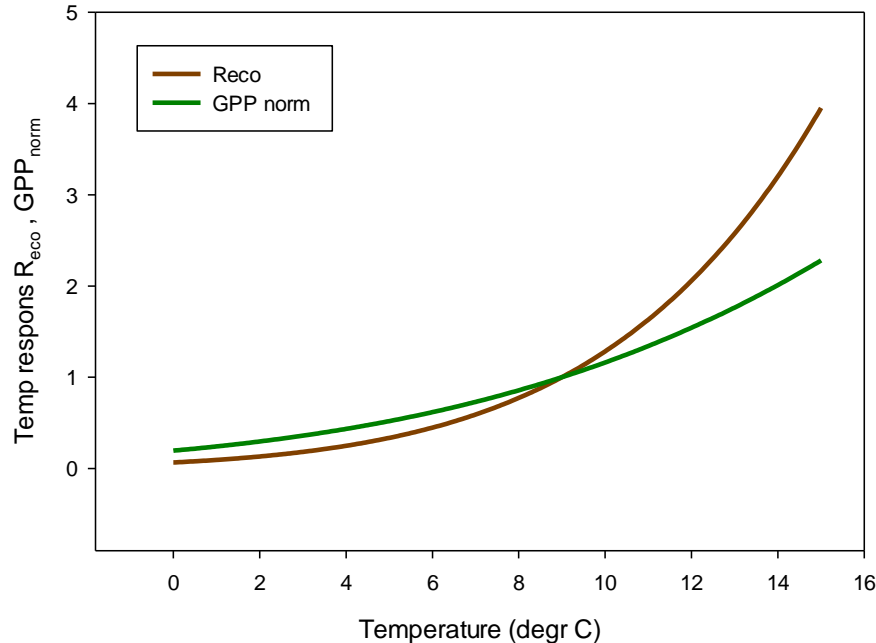


Figure 11. Temperature sensitivity for ecosystem respiration ( $R_{eco}$ ) (brown) and  $R_g$ -normalized (positive) gross primary productivity (GPP) (green).

In Fig. 11 we reversed the sign of the GPP temperature response function to make it more easily comparable with the  $R_{eco}$  response model. The temperature sensitivity ( $\mu\text{mol m}^{-2}\text{s}^{-1} \text{K}^{-1}$ ) can be estimated from the slope of these curves and the sensitivity is slightly higher for GPP than for  $R_{eco}$  in the interval 0 – 4.5 °C, thereafter the difference is small up to about 6 °C then it began to raise rapidly for  $R_{eco}$ . We tested what impact this could have by increasing the measured half-hourly air temperature by 1 °C and found that during the growing season the GPP increased by - 31.9  $\text{g C m}^{-2}$  and  $R_{eco}$  by 36.4  $\text{g C m}^{-2}$ . Thus, a slightly larger increase of  $R_{eco}$  as compared to GPP resulting in that the small sink of -2.5  $\text{gC m}^{-2}$  turns into a source of 4.5  $\text{gC m}^{-2}$ .

#### 4.5 $\text{CH}_4$ exchanges

The  $\text{CH}_4$  fluxes from the chamber measurements showed large variation over time (Fig. 12) and across sampling locations (Fig. 13). The mean  $\text{CH}_4$  flux of all samples was  $0.00051 \pm 0.00024 \mu\text{mol m}^{-2}\text{s}^{-1}$ . The uncertainty is given as the 95% confidence limit. Setting all fluxes that fell within the flux detection limits to zero changed the mean value with -0.2%. Assuming that the mean flux was representative for the whole of growing season 1, the total  $\text{CH}_4$  summer emission was 0.039 to 0.164  $\text{g CH}_4 \text{m}^{-2}$ .

We also noticed a clear trend during the summer with highest fluxes in mid-June and then decreasing during the following two sampling occasions. The respective mean values with 95% confidence intervals for the three sampling periods were  $0.00121 \pm 0.000512 \mu\text{mol m}^{-2}\text{s}^{-1}$  (June 14-15),  $0.000332 \pm 0.000465 \mu\text{mol m}^{-2}\text{s}^{-1}$  (June 26- July 2) and  $-0.00000781 \pm 0.0000936 \mu\text{mol m}^{-2}\text{s}^{-1}$  (August 25-26).

473 For CH<sub>4</sub> exchanges we found *ALD*,  $\theta$  and *GI* to contribute significantly to explain the variance of  
 474 the flux (Table 3). The CH<sub>4</sub> flux responded negatively to increasing *ALD* and positively to  $\theta$  and  
 475 *GI*.

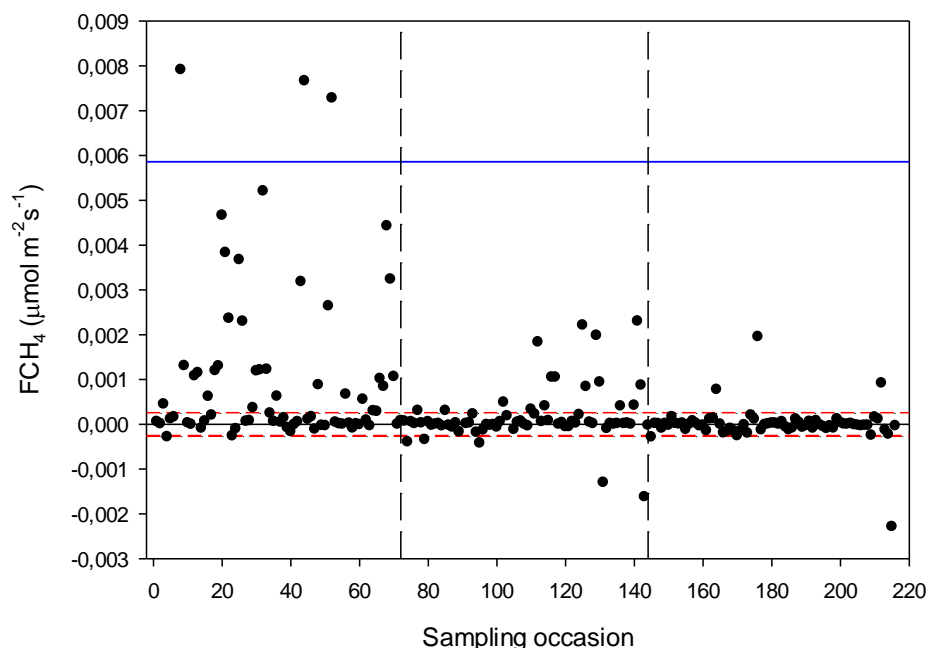
477 Table 3. Result of stepwise multiple linear regression with CH<sub>4</sub> flux as dependent variable.  
 478 Normality test failed but significance in all variables was confirmed with Wilcoxon Signed rank  
 479 tests. *ALD* is active layer depth,  $\theta$  is soil moisture and *GI* is green index.

480

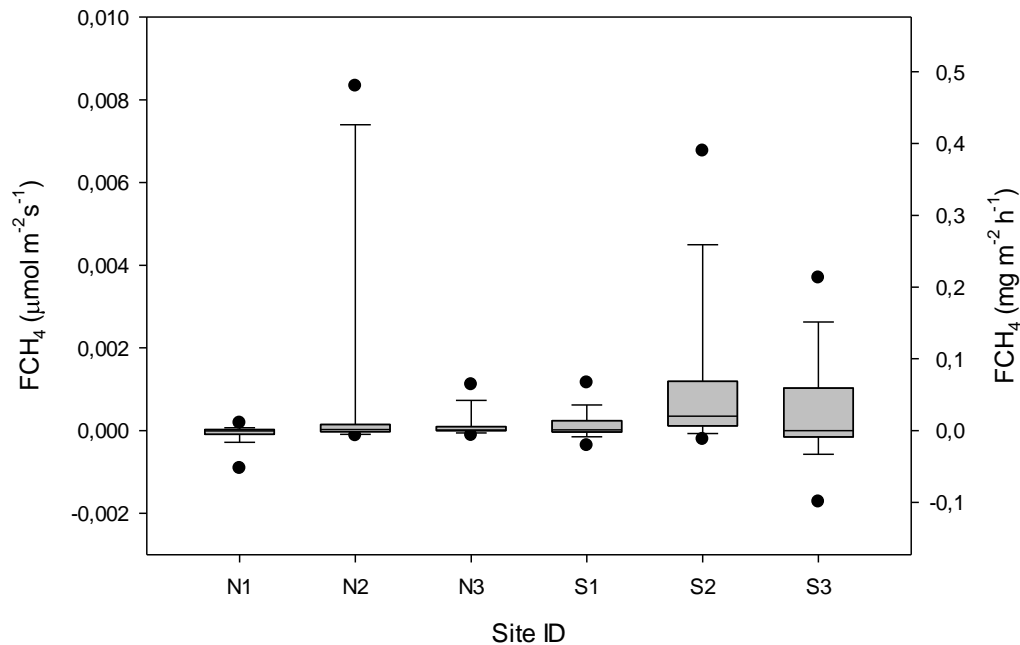
Variable	Delta-R <sup>2</sup>	Probability (p)
<i>ALD</i>	0.175	<0.001
$\theta$	0.025	0.01
<i>GI</i>	0.020	0.004

481

482



483  
 484 Figure 12. Measured CH<sub>4</sub> exchange (FCH<sub>4</sub>) from the 24 sampling points using dark chamber and  
 485 portable gas analyzer. The dashed red lines indicate CH<sub>4</sub> flux detection limit, (i.e. inside the  
 486 limits of detection the exact numbers are highly uncertain) and the blue line represents 3xS.D.  
 487 The dashed vertical lines – same as in Fig. 4.



488

489 Figure 13. Box plot of CH<sub>4</sub> fluxes (FCH<sub>4</sub>) per sampling location named N1-N3, S1-S3. The  
 490 statistics includes also the data that fall within the flux detection limits. The boundaries of the  
 491 grey boxes represent the 25% and 75% percentiles, the line represent the median, whiskers above  
 492 and below the boxes indicate the 10% and 90% percentiles. Outlying points are also shown.

## 493 5 Discussion

### 494 5.1 Seasonal CO<sub>2</sub> fluxes

495

496 We focus our discussion mainly on comparison with other tundra sites located in the North  
 497 Atlantic area since these sites are influenced by the North Atlantic Current with its impact on  
 498 weather patterns and climate. This limits the comparisons to sites in Greenland, Svalbard and  
 499 Northern Scandinavia. However, we broaden the comparison a bit by adding two sites from  
 500 Alaska.

501

502 Lund et al. (2012) found that the start of the uptake period was strongly correlated with start of  
 503 the snowmelt for the fen in Zackenberg, NE Greenland. They defined the start of snowmelt as  
 504 the day when snow depth was <0.1 m. This coincides very well with our definition of start of  
 505 growing season (see Fig. 2). Our results for the growing season NEE showing a small net uptake  
 506 of -2.5 g C m<sup>-2</sup> is at the low end in comparison with any other high arctic sites which all show a  
 507 larger gain of carbon during the growing seasons.

508

509 Lund et al. (2012) analysed 10 years of EC flux measurements from a heathland in Zackenberg  
 510 and they reported a NEE range of -39.7 to -4.3 g C m<sup>-2</sup> for the growing season. It was only two  
 511 years out of ten that showed NEE values close to zero but still indicating a small net uptake in  
 512 Zackenberg heath. Their measured growing season GPP was in the range of -95.4 to -54.1 g C m<sup>-2</sup>  
 513 and the R<sub>eco</sub> was in the range of 37.7 to 63.8 g C m<sup>-2</sup>. Our corresponding values were -112.7 g

514 C m<sup>-2</sup> for GPP and 110.2 g C m<sup>-2</sup> for R<sub>eco</sub>. López-Blanco et al. (2017) presented data over a  
515 period of eight years of EC flux measurements from Kobbefjord, SW Greenland over an area of  
516 mixed fen and heath vegetation. Their growing season ranges were; for NEE -74.2 to -45.9 g C  
517 m<sup>-2</sup>, for GPP -316.2 to -181.8 g C m<sup>-2</sup> and for R<sub>eco</sub> it was 144.2 to 279.2 g C m<sup>-2</sup> excluding 2011  
518 which was anomalous because of a pest outbreak and 2014 which did not have a full growing  
519 season.

520  
521 Our estimate of a small summer NEE of -11.8 g C m<sup>-2</sup> (Table 2) is also different in comparison  
522 with other tundra sites which show larger uptake during the summer; for a fen type of vegetation  
523 in NE Greenland Soegaard and Nordstroem (1999) reported -96.3 g C m<sup>-2</sup> while Rennermalm et  
524 al. (2005) reported -50 g C m<sup>-2</sup> for the same site but for a different year. Groendahl et al. (2007)  
525 reported a range of -1.4 to -18.9 g C m<sup>-2</sup> for heath vegetation also on NE Greenland.

526  
527 It is difficult to compare growing season values firstly because they are rarely defined the same  
528 way. Only small differences in definition of start and end of growing season can have a large  
529 impact on the NEE values since NEE is the sum of two large components of almost equal size  
530 and of different sign. Secondly, it is also difficult to compare GPP and R<sub>eco</sub> for any season since  
531 the methods to split NEE into components differ from case to case. The most reliable comparison  
532 is probably for summer season (June – August) since most studies represents this period best in  
533 terms of measurement coverage and quality. And thirdly, there are differences in vegetation type  
534 that can have a big impact on gas exchanges. Our moist moss tundra is dominated by moss  
535 species and mosses are not as efficient primary producers as vascular plants and this make the  
536 net uptake of carbon dioxide small as compared to heath or wet fen systems.

537  
538 The climate warming is predicted to be most evident at high latitudes such as the Arctic region.  
539 Svalbard has experienced significant warming during the last decades (1971-2017) with 3- 5  
540 degrees with the largest increase in the winter and smallest in the summer (Hanssen-Bauer et al.,  
541 2019). Our air temperature observations in 2015 are in line with these results (Fig.1). An  
542 interesting question is if such changes in temperature has also affected the net carbon balance of  
543 the ecosystem? Our analysis of temperature sensitivity of R<sub>eco</sub> and GPP shows that this could be  
544 the case for this site since R<sub>eco</sub> is increasing more than GPP for temperatures above about 6 °C  
545 which occurs quite frequent during the summer (see Fig. 2). Our analyses of the impact of a  
546 temperature increase of 1 °C showed that our small sink of -2.5 g C m<sup>-2</sup> during growing season  
547 would be turned into a similarly small source of 4.5 g C m<sup>-2</sup> for a 1 degree increase in air  
548 temperature. These results are in line of those of Welker et al. (2004) who performed a warming  
549 experiment in high Arctic tundra ecosystems. They showed that the net ecosystem exchange in  
550 the wet tundra ecosystem decreased by 20% during growing season under a 2 degree warming  
551 treatment. This was in contrast to the dry and mesic ecosystems which increased their net carbon  
552 uptake by 12-30%.

553

554

## 555 5.2 CH<sub>4</sub> fluxes

556

557 Our estimated growing season CH<sub>4</sub> flux of 0.08 g C m<sup>-2</sup> is very low compared to most other  
558 methane emitting tundra sites; the Zackenberg fen site emitted CH<sub>4</sub> in the range 1.4 to 4.9 g C m<sup>-2</sup>  
559 (Mastepanov et al. (2013), Jackowicz-Korczynski et al. (2010) and Jammet et al. (2015)

560 reported 20.1 to 25.1 g CH<sub>4</sub> m<sup>-2</sup> for the Stordalen mire in Northern Sweden. For three different  
561 sites in northern Alaska, Bao et al. (2021) reported annual emissions between 1.8 and 8.5 g CH<sub>4</sub>  
562 m<sup>-2</sup> which corresponds to 0.94 and 4.5 g CH<sub>4</sub> m<sup>-2</sup> for the growing season based on their estimate  
563 that growing season emissions are 52.6% of the annual emissions. Sachs et al. (2008) measured  
564 CH<sub>4</sub> exchanges with EC method in a northern Siberian polygon tundra and found generally low  
565 fluxes of about 18.5 mg CH<sub>4</sub> m<sup>-2</sup> day<sup>-1</sup> with little variation over the growing season. This rate  
566 adds up to 2.3 g CH<sub>4</sub> m<sup>-2</sup> for their four months long growing season.

567  
568 It should be pointed out that we did not perform measurements during the shoulder seasons  
569 meaning that we probably underestimate the seasonal total. Importance of shoulder seasons was  
570 first pointed out by Mastepanov et al. (2008) which discovered a large burst of CH<sub>4</sub> at and after  
571 the onset of soil freezing. One interesting observation is that the main part of our CH<sub>4</sub> flux  
572 occurred during the sampling period 14-15 June 2016 which is about 30 days after snow melt.  
573 This is the time of the season when CH<sub>4</sub> emissions normally are peaking (Mastepanov et al.  
574 2013). After that, the rates dropped to practically zero in late August (see Fig. 12).

575  
576  
577 The comparison between the different sites are hampered by the fact that they in most cases  
578 belong to different bioclimatic subzones with differences in climate and vegetation (Walker et  
579 al., 2005). The only site besides Kapp Linne that belong to subzone B is the one in Ny Ålesund.  
580 The other high Arctic sites Adventdalen and Zackenberg both belong to subzone C, the  
581 intermediate high/low Arctic sites Kobbefjord and Disco Island belongs to subzone D  
582 respectively C/D. The low Arctic site Atqasuk belong to subzone D and the Imnavait Creek  
583 belong to subzone E. The sub-Arctic Abisko is not classified by Walker et al. (2005) but based  
584 mean July air temperature it should belong to subzone E. These differences in climate and  
585 vegetation should be kept in mind when comparing results from different sites.

### 586 587 5.3 Environmental controls of fluxes

588  
589 A key issue in high Arctic is how ecosystems with soil that contain large amounts of frozen  
590 carbon will respond to warming. A recent report about the future climate of Svalbard (Hanssen-  
591 Bauer et al. 2019) show that appalling changes are at risk to occur. By 2071-2100 compared to  
592 1971-2000 the mean annual temperature is estimated to increase by 7 °C to 10 °C for the medium  
593 and high emission scenarios, respectively. Precipitation is also estimated to increase by 45%  
594 respectively 65% for these scenarios. Such large changes will of course also have a lot of other  
595 impacts as well for instance shorter snow season, more erosion and sediment transport, changes  
596 in vegetation composition and growth etc etc. Assessment of such large changes are very  
597 difficult and is far beyond the scope of this paper. We have however shown that for a smaller  
598 temperature increase of 1 degree, the impact on the net carbon balance during the growing  
599 season will be minute; the increase in ecosystem respiration is compensated for by a  
600 corresponding, or actually slightly larger increase of gross primary productivity. Similar  
601 compensation effect was obtained for a heath site in Zackenberg by Lund et al. (2012). They  
602 used multi-year measurements to assess the effect of changes in temperature on the growing  
603 season fluxes

604

605 We found that air temperature was the main control of ecosystem respiration followed by soil  
606 moisture and greenness index (Table 1). We had expected that soil temperature should contribute  
607 significantly to explain the variations in  $R_{eco}$  but it did not. Cannone et al. (2019) showed that  
608 ground surface temperature at 2 cm depth contributed significantly to explain  $R_{eco}$  in nearby  
609 Adventdalen during early, peak and late parts of the growing season. In their study soil moisture  
610 was also significant during peak and late seasons. One possible explanation to this difference in  
611 responses could be that our soil temperature was measured at 5 cm depth and that air temperature  
612 was more representative for the microbial processes taking place in or near the soil surface.  
613 Interestingly, GI contributed significantly to explain variations in  $R_{eco}$ . The GI was clearly  
614 correlated with the abundance of *Salix polaris* (see Supplement) and thus we interpret the  
615 positive correlation between GI and  $R_{eco}$  to be an effect of increasing contribution by autotrophic  
616 respiration to the total respiration.

617 We found no significant correlation between  $CH_4$  emission and temperature. The best  
618 explanation was by active layer depth followed by soil moisture and GI (Table 3). But it should  
619 be pointed out that ALD and  $\theta$  are not independent from each other and that ALD can be  
620 regarded as a proxy for any seasonal variability, like plant phenology. Soil moisture decreases  
621 with increasing active layer depth. The correlation between GI and  $CH_4$  emission is probably  
622 also connected with abundance of the vascular plant *Salix polaris*. Vascular plants are since long  
623 mentioned as a pathway for  $CH_4$  from the soil interior to the atmosphere in wet tundra  
624 ecosystems (e.g. Schimel, 1995) but it could also be an effect of mediation of soil by the root  
625 exudation of organic acids as mentioned by Ström et al. (2012). However, we have not found any  
626 studies supporting the latter hypothesis concerning *Salix polaris*.

## 627 **6 Conclusions**

628 Our analyses of EC and chamber flux measurements have shown that the moss tundra on Kapp  
629 Linne is a small sink of  $CO_2$  and a small source of  $CH_4$  during the growing season. Realizing that  
630 the winter season also emit  $CO_2$ , we tentatively conclude that this moist moss tundra is a source  
631 on an annual basis. Concerning the magnitude of the  $CO_2$  exchanges during summer we find it to  
632 be anomalous compared to fens and heath ecosystems located in the North Atlantic region  
633 which all are sinks during the summer. The  $CH_4$  exchange is much lower than for other tundra  
634 ecosystems in the region.

635  
636 The temperature sensitivity for  $CO_2$  exchange was slightly higher for GPP than for  $R_{eco}$  in the  
637 low temperature range of 0-4.5 °C, almost similar up to 6 °C and thereafter it was considerably  
638 higher for  $R_{eco}$ . The consequence of this, for a small increase in air temperature of 1 degree (all  
639 other variables assumed unchanged) was that the respiration increased more than photosynthesis  
640 turning the small sink into a small source. But a warmer winter period would probably also result  
641 in an additionally increased loss of carbon. We cannot rule out that the reason why the moss  
642 tundra is close to balance today is an effect of the warming that has already taken place in  
643 Svalbard.

644 The analysis of which environmental factors that controlled the small-scale fluxes showed that  
645 air temperature dominated for  $R_{eco}$  and active layer depth for  $CH_4$  but we also found that  
646 greenness index significantly explained part of the variation in these fluxes. For  $R_{eco}$  we  
647 attributed this to an increased share of autotrophic respiration to the total and for  $CH_4$  we

648 hypothesized that the abundance of the dwarf shrub *Salix polaris* effected the exchange either  
649 through internal plant pathway for methane or through increased provision of C substrate to the  
650 anaerobic microbial community stimulating the production of methane. This finding is an  
651 indication that modeling of CO<sub>2</sub> as well as of CH<sub>4</sub> fluxes can be improved by also considering  
652 differences and changes in greenness of the vegetation.

## 653 **7 Supplement**

654 The supplement contains some additional photographs of equipment, site and color photographs  
655 of vegetation within the frames used for chamber measurements.

## 656 **8 Data availability**

657 Data can be obtained from <https://zenodo.org> ([10.5281/zenodo.5704508](https://zenodo.org/record/10.5281/zenodo.5704508)).

## 658 **9 Author contribution**

659 AL designed the study and wrote the manuscript. NP and AL performed the EC measurements  
660 and analysed the EC data. ISJ did the vegetation characterization. AL, CS, LK and MBN  
661 performed the chamber measurements. All authors have read and commented the manuscript.

## 662 **10 Competing interests**

663 We declare no competing interests.

## 664 **11 Acknowledgments**

665 This work did not receive any other funding except salaries for the authors from their respective  
666 organizations. Observations of air temperature, relative humidity, precipitation, ground ice  
667 conditions and snow depth were obtained from Norwegian Centre for Climate Services (NCCS)  
668 and provided under licence CC BY 4.0. Global radiation data from Adventdalen was obtained  
669 from the University Centre in Svalbard (UNIS). Thanks to associated professor Jonas Åkerman,  
670 Lund University for support with information about the site.

671

## 672 **12 References**

673 Arias, P. A., Bellouin, E., Coppola, R.G. et al.: Technical Summary, in: Climate Change 2021:  
674 The Physical Science Basis. Contribution of Working Group I to the Sixth Assessment  
675 Report of the Intergovernmental Panel on Climate Change, edited by: Masson-Delmotte,  
676 V., P. Zhai, A. Pirani, S. L. Connors, C. Péan, S. Berger, N. Caud, Y. Chen, L. Goldfarb,  
677 M. I. Gomis, M. Huang, K. Leitzell, E. Lonnoy, J.B.R. Matthews, T. K. Maycock, T.  
678 Waterfield, O. Yelekçi, R. Yu and B. Zhou, Cambridge University Press, In Press, 2021.

679 Bao, T., Xu, X., Jia, G., Billesbach, D.P. and Sullivan, R.C.: Much stronger tundra methane  
680 emissions during autumn freeze than spring thaw, *Global Change Biology*, 27, 376–387,  
681 [https://doi.org/ 10.1111/gcb.15421](https://doi.org/10.1111/gcb.15421), 2021

682 Bosiö, J., Stiegler, C., Johansson, M., Mbufong, H. N. and Christensen, T. R.: Increased  
683 photosynthesis compensates for shorter growing season in subarctic tundra—8 years of



- 684 snow accumulation manipulations, *Climatic Change*, 127, 321–334,  
685 <http://doi.org/10.1007/s10584-014-1247-4>, 2014.
- 686 Burba, G. G., McDermitt, D., Grelle, A., Anderson, D.J. and Xu, L.: Addressing the influence of  
687 instrument surface heat exchange on the measurements of CO<sub>2</sub> flux from open-path gas  
688 analyzers, *Global Change Biology*, 14, 1854–1876, [https://doi.org/10.1111/j.1365-](https://doi.org/10.1111/j.1365-2486.2008.01606.x)  
689 [2486.2008.01606.x](https://doi.org/10.1111/j.1365-2486.2008.01606.x), 2008.
- 690 Callaghan, T.V., Björn, L O., Chapin III, F.S., Chernov, Y., Christensen, T.R., Huntley, B., Ims,  
691 R., Johansson, M., Jolly Riedlinger, D., Jonasson, S., Matveyeva, N., Oechel, W.,  
692 Panikov, N. and Shaver, G.: Arctic tundra and polar desert ecosystems, in: *Arctic Climate*  
693 *Impact Assessment*, edited by: ACIA, Cambridge University Press, 243-352, 2005.
- 694 Cannonea, N., Pontib, S., Christiansen, H.H., Christensen, T.R., Pirk, N. and Guglielmin, M.:  
695 Effects of active layer seasonal dynamics and plant phenology on CO<sub>2</sub> land atmosphere  
696 fluxes at polygonal tundra in the High Arctic, Svalbard, *Catena*, 174, 142-153,  
697 <https://doi.org/10.1016/j.catena.2018.11.013>, 2019.
- 698 Christensen, T.R., Johansson, T., Akerman, H.J. and Mastepanov, M.: Thawing sub-arctic  
699 permafrost: Effects on vegetation and methane emissions, *Geophysical Research Letters*,  
700 31, L04501, <https://doi.org/10.1029/2003GL018680>, 2004.
- 701 Christensen, T.R., Jackowicz-Korzynski, M., Aurela, M., Crill, P., Heliasz, M., Mastepanov, M.  
702 and Friborg, T.: Monitoring the Multi-Year Carbon Balance of a Subarctic Palsa Mire  
703 with Micrometeorological Techniques, *Ambio*, 41, 207–217,  
704 <https://doi.org/10.1007/s13280-012-0302-5>, 2012.
- 705 Dobler, A., Lutz, J., Landgren, O. and Haugen, J. E.: Circulation Specific Precipitation Patterns  
706 over Svalbard and Projected Future Changes, *Atmosphere*, 11, 1378;  
707 [doi:10.3390/atmos11121378](https://doi.org/10.3390/atmos11121378), 2021.
- 708
- 709 Euskirchen, E. S., Bret-Harte, M. S., Scott, G. J., Edgar, C., and Shaver, G. R.: Seasonal patterns  
710 of carbon dioxide and water fluxes in three representative tundra ecosystems in northern  
711 Alaska, *Ecosphere*, 3, 1–19, <https://doi.org/10.1890/ES11-00202.1>, 2012.
- 712
- 713 Euskirchen, E.S., Bret-Harte, M.S., Shaver, G.R., Edgar, C.W., and Romanovsky, V.E.: Long-  
714 Term Release of Carbon Dioxide from Arctic Tundra Ecosystems in Alaska, *Ecosystems*,  
715 20, 960–974, <http://doi.org/10.1007/s10021-016-0085-9>, 2017.
- 716 Friedlingstein, P., Cox, P., Betts, R., Bopp, L., von Bloh, W., Brovkin, V., Cadule, P., Doney, S.,  
717 Eby, M., Fung, I., Bala, G., John, J., Jones, C., Joos, F., Kato, T., Kawamiya, M., Knorr,  
718 W., Lindsay, K., Matthews, H. D., Raddatz, T., Rayner, P., Reick, C., Roeckner, E.,  
719 Schnitzler, K. G., Schnur, R., Strassmann, K., Weaver, A. J., Yoshikawa, C., and Zeng,

720 N.: Climate-carbon cycle feedback analysis: Results from the C4MIP model  
721 intercomparison, *J. Climate*, 19, 3337–3353, <https://doi.org/10.1175/JCLI3800.1>, 2006.

722 Friedlingstein, P., O’Sullivan, M., Jones, M.W. et al.: Global carbon budget 2010, *Earth Syst.*  
723 *Sci. Data*, 12, 3269–3340, <https://doi.org/10.5194/essd-12-3269-2020>, 2019.

724 Groendahl, L., Friborg, T., and Soegaard, H.: Temperature and snow-melt controls on  
725 interannual variability in carbon exchange in the high Arctic, *Theor. Appl. Climatol.*, 88,  
726 111–125, <http://doi.org/10.1007/s00704-005-0228-y>, 2007.

727 Hanssen-Bauer, I., Førland, E.J., Hisdal, H., Mayer, S., Sandø, A.B. and Sorteberg, A.: Climate in  
728 Svalbard 2100 – a knowledge base for climate adaptation, Norwegian Environment  
729 Agency, Report no. 1/2019., 2019.

730 Hugelius, G., Strauss, J., Zubrzycki, S., Haren, J.W., Schuur, E.A.G., Ping, C.-L., Schirrmeyer,  
731 L., Grosse, G., Michaelson, G.J., Koven, C.D., O’Donnell, J.A., Elberling, B., Mishra,  
732 U., Camill, P., Yu, Z., Palmtag, J. and Kuhry, P.: Estimated stocks of circumpolar  
733 permafrost carbon with quantified uncertainty ranges and identified data gaps,  
734 *Biogeosciences*, 11, 6573–6593, <http://doi.org/10.5194/bg-11-6573-2014>, 2014.

735 Jackowicz-Korczynski, M., Christensen, T. R., Backstrand, K., Crill, P., Friborg, T.,  
736 Mastepanov, M. and Strom, L.: Annual cycle of methane emission from a subarctic  
737 peatland, *J. Geophys. Res.-Biogeo.*, 115, G02009, <http://doi.org/10.1029/2008JG000913>,  
738 2010.

739 Jammet, M., Crill, P., Dengel, S. and Friborg, T.: Large methane emissions from a subarctic  
740 lake during spring thaw: Mechanisms and landscape significance. *J. Geophys. Res.-*  
741 *Biogeo.*, 120, 2289-2305, <http://doi.org/10.1002/2015JG003137>, 2015.

742 Kljun, N., Calanca, P., Rotach, M.W., and Schmid, H.P.: A simple two-dimensional  
743 parameterisation for Flux Footprint Prediction (FFP), *Geosci. Model Dev.*, 8, 3695-3713,  
744 <http://doi.org/10.5194/gmd-8-3695-2015>, 2015.

745 Lasslop, G., Reichstein, M., Papale, D., Richardson, A., Arneth, A., Barr, A., Stoy, P. and  
746 Wohlfahrt, G.: Separation of net ecosystem exchange into assimilation and respiration  
747 using a light response curve approach: critical issues and global evaluation. *Global*  
748 *Change Biology*, 16, 187-208, <https://doi.org/10.1111/j.1365-2486.2009.02041.x>, 2010.

749 Li-Cor: EddyPro® Software (Version 6.0), Li-Cor Inc., Lincoln, USA, 2016.

750 Lloyd, J., and Taylor, J.A.: On the temperature dependence of soil respiration, *Functional*  
751 *Ecology*, 8(3), 315-323, 1994.

752 Lopez-Blanco, E., Lund, M., Williams, M., Tamstorf, M.P., Westergaard-Nielsen, A., Exbrayat,  
753 J.-F., Hansen, B.U., and Christensen, T.R.: Exchange of CO<sub>2</sub> in Arctic tundra: impacts of

- 754 meteorological variations and biological disturbance, *Biogeosciences*, 14, 4467–4483,  
755 <https://doi.org/10.5194/bg-14-4467-2017>, 2017.
- 756 Lund, M., Falk, J. M., Friborg, T., Mbufong, H. N., Sigsgaard, C., Soegaard, H., and Tamstorf,  
757 M. P.: Trends in CO<sub>2</sub> exchange in a high Arctic tundra heath, 2000–2010, *J. Geophys.*  
758 *Res.- Biogeo.*, <https://doi.org/10.1029/2011JG001901>, 2012.
- 759 Lüers, J., Westermann, S., Piel, K., and Boike, J.: Annual CO<sub>2</sub> budget and seasonal CO<sub>2</sub>  
760 exchange signals at a high Arctic permafrost site on Spitsbergen, Svalbard archipelago,  
761 *Biogeosciences*, 11, 6307–6322, <http://doi.org/10.5194/bg-11-6307>, 2014.
- 762 Mastepanov, M., Sigsgaard, C., Dlugokencky, E. J., Houweling, S., Strom L., Tamstorf, M. P.,  
763 and Christensen, T. R.: Large tundra methane burst during onset of freezing, *Nature*, 456,  
764 628–631, <http://doi.org/10.1038/nature07464>, 2008.
- 765 Mastepanov, M., Sigsgaard, C., Tagesson, T., Ström, L., Tamstorf, M. P., Lund, M., and  
766 Christensen, T. R.: Revisiting factors controlling methane emissions from high-Arctic  
767 tundra, *Biogeosciences*, 10, 5139–5158, <https://doi.org/10.5194/bg-10-5139-2013>, 2013.
- 768 McGuire, A. D., Christensen, T. R., Hayes, D., Heroult, A., Euskirchen, E., Kimball, J. S.,  
769 Koven, C., Lafleur, P., Miller, P. A., Oechel, W., Peylin, P., Williams, M., and Yi, Y.: An  
770 assessment of the carbon balance of Arctic tundra: comparisons among observations,  
771 process models, and atmospheric inversions, *Biogeosciences*, 9, 3185–3204,  
772 <https://doi.org/10.5194/bg-9-3185-2012>, 2012.
- 773 Myers-Smith, I. H., Kerby, J. T., Phoenix, G. K., Bjerke, J. W., Epstein, H. E., Assman, J. J.,  
774 John, C., Adreu-Hayles, L., Angers-Blondin, S., Beck, P. S. A., Berner, L. T., Bhatt, U.  
775 S., Bjorkman, A. D., Blok, D., Bryn, A., Christiansen, C. T., Cornelissen, J. H. C.,  
776 Cunliffe, A. M., Elmendorf, S. C., Forbes, B. C., Goetz, S. J., Hollister, R. D., de Jong,  
777 R., Loranty, M. M., Marcias-Fauria, K., Maseyk, K., Normand, S., Olofsson, J., Parker,  
778 T. C., Parmentier, F.-J. W., Post, E., Schaepman-Strub, G., Stordal, F., Sullivan, P. F.,  
779 Thomas, H. J. D., Tømmervik, H., Treharne, R., Tweedie, C. E., Walker, D. A.,  
780 Wilmking, M. and Wipf, S.: Complexity revealed in the greening of the Arctic, *Nat.*  
781 *Clim. Chang.*, 10, 106–117, <https://doi.org/10.1038/s41558-019-0688>, 2020.
- 782 Oechel, W. C., C. A. Laskowski, G. Burba, B. Gioli, and Kalhori, A.A.M.: Annual patterns and  
783 budget of CO<sub>2</sub> flux in an Arctic tussock tundra ecosystem, *J. Geophys. Res. Biogeo.*,  
784 119, 323–339, <http://doi.org/10.1002/2013JG002431>, 2014.
- 785 Pastorello, G., Trotta, C., Canfora, E. et al.: The FLUXNET2015 dataset and the ONEFlux  
786 processing pipeline for eddy covariance data, *Sci Data*, 7, 225,  
787 <https://doi.org/10.1038/s41597-020-0534-3>, 2020.
- 788 Pirk, N., Sievers, J., Mertes, J., Parmentier, F.-J. W., Mastepanov, M., and Christensen, T. R.:  
789 Spatial variability of CO<sub>2</sub> uptake in polygonal tundra: assessing low-frequency

- 790 disturbances in eddy covariance flux estimates, *Biogeosciences*, 14, 3157–3169,  
791 <https://doi.org/10.5194/bg-14-3157-2017>, 2017.
- 792 Post, E., Forchhammer, M. C., Bret-Harte, M. S., Callaghan, T. V., Christensen, T. R., Elberling,  
793 B., Fox, A. D., Gilg, O., Hik, D. S., Høye, T. T., Ims, R. A., Jeppesen, E., Klein, D. R.,  
794 Madsen, J., McGuire, A. D., Rysgaard, S., Schindler, D. E., Stirling, I., Tamstorf, M. P.,  
795 Tyler, N. J. C., van der Wal, R., Welker, J., Wookey, P. A., Schmidt, M. and Astrup, P.:  
796 Ecological dynamics across the arctic associated with recent climate change, *Science*,  
797 325, 1355–1358, <http://doi.org/10.1126/science.1173111>, 2009.
- 798 Ravolainen, V., Soininen, E. M., Jónsdóttir, I. S., Eischeid, I., Forchhammer, M., van der Wal,  
799 R. and Pedersen, A. Ø.: High Arctic ecosystem states: Conceptual models of vegetation  
800 change to guide long-term monitoring and research, *Ambio*, 49, 666–677,  
801 <https://doi.org/10.1007/s13280-019-01310-x>, 2020.
- 802 Rennermalm, A.K., Soegaard, H., and Nordstroem, C.: Interannual Variability in Carbon  
803 Dioxide Exchange from a High Arctic Fen Estimated by Measurements and Modeling,  
804 *Arctic, Antarctic, and Alpine Research*, 37(4), 545-556, [https://doi.org/10.1657/1523-0430\(2005\)037\[0545:IVICDE\]2.0.CO;2](https://doi.org/10.1657/1523-0430(2005)037[0545:IVICDE]2.0.CO;2), 2005.
- 806 Richardson, A. D., Braswell, B. H., Hollinger, D. Y., Jenkins, J. P. and Ollinger, S. V.: Near-  
807 surface remote sensing of spatial and temporal variation in canopy phenology, *Ecological*  
808 *Applications*, 19, 1417–1428, <http://doi.org/10.1890/08-2022.1>, 2009.
- 809 Sachs, T., Wille, C., Boike, J., and Kutzbach, L.: Environmental controls on ecosystem-scale  
810 CH<sub>4</sub> emission from polygonal tundra in the Lena river delta, Siberia, *J. Geophys. Res.-*  
811 *Biogeosci.*, 113, G00A03, <http://doi.org/10.1029/2007JG000505>, 2008.
- 812 Saunio, M., Stavert, A.R., Poulter, B et al.: The global methane budget 2000-2017, *Earth Syst.*  
813 *Sci. Data*, 12, 1561–1623, <https://doi.org/10.5194/essd-12-1561>, 2020.
- 814 Schimel, J.P.: Plant Transport and Methane Production as Controls on Methane Flux from Arctic  
815 Wet Meadow Tundra, *Biogeochemistry*, 28 (3), 183-200,  
816 <https://doi.org/10.1007/BF02186458>, 1995.
- 817 Schuur, E. A. G., McGuire, A. D., Schadel, C., Grosse, G., Harden, J. W., Hayes, D. J.,  
818 Hugelius, G., Koven, C. D., Kuhry, P., Lawrence, D. M., Natali, S. M., Olefeldt, D.,  
819 Romanovsky, V. E., Schaefer, K., Turetsky, M. R., Treat, C. C., and Vonk, J. E.: Climate  
820 change and the permafrost carbon feedback, *Nature*, 520, 171–179,  
821 <https://doi.org/10.1038/nature14338>, 2015.
- 822 Soegaard, H. & Nordstroem, C.: Carbon dioxide exchange in a high-arctic fen estimated by eddy  
823 covariance measurements and modeling, *Glob. Change Biol.*, 5, 547–562,  
824 <https://doi.org/10.1111/j.1365-2486.1999.00250.x>, 1999.

- 825 Strom, L., Tagesson, T., Mastepanov, M., and Christensen, T. R.: Presence of *Eriophorum*  
826 *scheuchzeri* enhances substrate availability and methane emission in an Arctic wetland,  
827 *Soil Biol. Biochem.*, 45, 61–70, <http://doi.org/10.1016/j.soilbio.2011.09.005>, 2012.  
828
- 829 Walker, D. A., Raynolds, M. K., Daniëls, F. J. A., Einarsson, E., Elvebakk, A., Gould, W. A.,  
830 Katenin, A. E., Kholod, S. S., Markon, C. J., Melnikov, E. S., Moskalenko, N. G., Talbot,  
831 S. S., Yurtsev, B. A. and the other members of the CAVM Team: The Circumpolar  
832 Arctic vegetation map, *Journal of Vegetation Science*, 16, 267-282,  
833 <https://doi.org/10.1111/j.1654-1103.2005.tb02365.x>, 2005.
- 834 Welker, J.M., Fahnestock, J.T., Henry, G.H.R., O’Dea, K.W. and Chimner, R.A.: CO<sub>2</sub> exchange  
835 in three Canadian High Arctic ecosystems: response to long-term experimental warming.  
836 *Global Change Biology*, 10, 1981-1995. Doi: 1011/j.1365-2486.2004.00857.x, 2004.  
837
- 838 Vanderpuye, A. W., Elvebakk, A. and Nilsen, L.: Plant communities along environmental  
839 gradients of high-arctic mires in Sassendalen, Svalbard, *J. Veg. Sci.*, 13, 875–884,  
840 <http://doi.org/10.1111/j.1654-1103.2002.tb02117.x>, 2002.  
841
- 842 Vickers, H., Karlsen, S. R. and Malnes, E.: A 20-Year MODIS-Based Snow Cover Dataset for  
843 Svalbard and Its Link to Phenological Timing and Sea Ice Variability, *Remote Sens.*, 12,  
844 1123; doi:10.3390/rs12071123, 2020.  
845  
846
- 847 Wutzler, T., Lucas-Moffat, A., Migliavacca, M., Knauer, J., Sickel, K., Šigut, L., Menzer, O. and  
848 Reichstein, M.: Basic and extensible post-processing of eddy covariance flux data with  
849 REddyProc, *Biogeosciences*, 15(16), 5015-5030, Doi:10.5194/bg-15-5015-2018, 2018.
- 850 Zhang, W., Jansson, P-E., Sigsgaard, C., McConnella, A., Jammet, M.M., Westergaard-Nielsen,  
851 A., Lund, M., Friberg, T., Michelsen, A., and Elberling, B.: Model-data fusion to assess  
852 year-round CO<sub>2</sub> fluxes for an arctic heath ecosystem in West Greenland (69°N),  
853 *Agricultural and Forest Meteorology*, 272-273, 176-186,  
854 <https://doi.org/10.1016/j.agrformet.2019.02.021>, 2019.